JOURNAL OF MATERIALS SCIENCE **34** (1999) 2039–2047

An iteration method for directly determining *J*-Resistance curves of nuclear structural steels

THAK-SANG BYUN, BONG-SANG LEE, JI-HYUN YOON, JUN-HWA HONG
Reactor Materials Department, Korea Atomic Energy Research Institute, P.O. Box 105, Yusong, Taejon 305-600, South Korea
E-mail: bongsl@nanum.kaeri.re.kr

An iteration method has been developed for determining crack growth and fracture resistance curves (*J*-*R* curves) of nuclear structural steels from the load versus load-line displacement record only. In this method, the hardening curve, the load versus displacement curve at a given crack length, is assumed to be a power-law function, where the exponent varies with the crack length. The exponent is determined by an iterative calculation method with the assumption that the exponent varies linearly with the load-line displacement. The proposed method was applied to the static *J*-*R* tests using compact tension (CT) specimens, a three-point bend (TPB) specimen, and a cracked round bar (CRB) specimen as well as it was applied to the quasi-dynamic *J*-*R* tests using CT specimens. The *J*-*R* curves determined by the proposed method were compared with those obtained by the conventional testing methodologies. The results showed that the *J*-*R* curves could be determined directly by the proposed iteration method with sufficient accuracy in the specimens from SA508 and SA516 pressure vessel steels and their welds and SA312 stainless steel.

1. Introduction

Since the *J*-integral has been regarded as the most important parameter for characterizing the elastic-plastic fracture resistance of structural materials, significant efforts have been devoted to develop more simplified methodologies of determining *J*-integral versus crack extension curve (*J*-*R* curve) [1–21]. In the *J*-*R* fracture testing the crack length measurement is the most cumbersome procedure and needs a high degree of accuracy to obtain a correct *J*-*R* curve. The most successful experimental methods using a single specimen are the elastic unloading compliance method and potential drop method [22, 23]. In static fracture testing they are now used routinely in many laboratories. However, the unloading compliance method can not be applied to the dynamic loading conditions because the unloading-reloading cycles to obtain the elastic compliance need a quasi-static loading condition. Also, the potential drop method requires much sophisticated equipment such as a high current power supplier and a high-speed data acquisition system, and there is a difficulty in determining the crack growth initiation point in dynamic fracture testing.

To eliminate these limitations in the experimental measurement of crack length, several direct methods have been attempted to obtain the *J*-*R* curve from the load versus displacement record only without additional equipment. The most important approaches are the key curve method [2–5], normalization method [6–15], and load ratio method [16–18]. The key curve method is based on the assumption that the load is independent of the crack growth history and can be defined by a definite function of load line displacement and crack length. The crack length can be expressed as a functional of the key curve function, its partial derivatives, and load-displacement data. For a given material, a unique 'key curve' is assumed to exist, and the curve function is obtained by multi-specimen testing or computer calculation [2].

The normalization method was developed based on the similar concept of the key curve method. However, this method uses individual normalized curves for each test itself rather than using a universal key curve for the given material. One important point of this method is that the separation of variables, crack length and displacement, is applied to the expression for load. Thus the normalized load is given as a function of displacement only. The power-law function [10–12] or three parameter function [13–15], so-called LMN function, has been frequently used as the normalization function form.

In the load ratio method, a reference hardening curve (a load versus displacement curve without crack extension) is needed to obtain the amount of crack extension [16–18]. It is assumed that at a given total displacement the same plastic displacement is assumed for the reference-hardening curve and experimental load versus displacement curve. Then the elastic unloading compliance is determined for each curve, and therefore the crack length can be calculated using the relationship between the elastic unloading compliance and the crack length.

In the previous direct methods, the final result depends on how to determine the required curves; such as the key curve, normalization function, reference-hardening curve. To obtain more accurate curves, many modified methods have been suggested and successfully applied to various materials [3, 14, 15, 17, 18]. We tried to develop an alternate direct method for determining J-R curves from load versus displacement data. This paper presents the new direct method (we call it 'iteration method') which can be applied to various types of specimen and to any loading rate. For a given crack length, the hardening curve is expressed by a power-law function of total displacement. Changing the constants in the power-law function approximates the variation of hardening curve with the crack growth. The exponent of the hardening curve is expressed as a linear function of displacement and is determined by iterative calculations. The other constants are directly obtained from the experimental load versus displacement data. As a result, the iteration method can be applied to any specimen type as long as the J-integral is formulated for the specimen. For each case, the amounts of crack growth between data points are calculated based on the calculated power-law hardening curves, and then the J-R curve is determined. This paper includes the application results for CT specimen cases including static tests and quasi-dynamic tests and the results for the three-point bend (TPB) specimen and cracked round bar (CRB) specimen cases.

2. Iteration method

2.1. Basic formulation

According to the definition of energy release rate [24], the J-integral is expressed as

$$J = -\frac{1}{B}\frac{\partial U}{\partial a}\bigg|_{v=\text{const}}, \tag{1}$$

where B is the specimen thickness, a is the crack length, v is the load-line displacement, and U is the elastic-plastic energy measured as the area under the hardening curve. The experimental load versus displacement curve and hardening curves are illustrated in Fig. 1. For a fixed displacement v_i, the difference between the energies for the crack lengths a_i and a_{i+1} is given by

$$-\Delta U_i = U_i - U_{i+1} = U_i(1 - R_i), \tag{2}$$

where the energies, U_i and U_{i+1}, are the area under the hardening curves for a_i and a_{i+1}, respectively:

$$U_i = \int_0^{v_i} P(a_i, v)\,\mathrm{d}v, \tag{3a}$$

$$U_{i+1} = \int_0^{v_i} P(a_{i+1}, v)\,\mathrm{d}v, \tag{3b}$$

and R_i is the ratio between the energies; $R_i = U_{i+1}/U_i$. If the adjacent data points in the experimental load-displacement curve are spaced close enough that Δa_i is small, the partial derivative in Equation 1 is close to $\Delta U_i/\Delta a_i$. Then the amount of crack extension, Δa_i $(=a_{i+1} - a_i)$, is approximated by

$$\Delta a_i = \frac{U_i(1 - R_i)}{B J_i}. \tag{4}$$

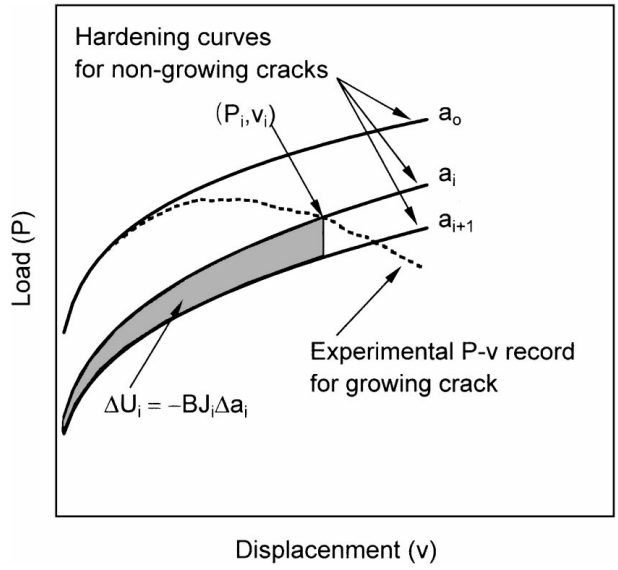

Figure 1 Schematic of experimental load versus displacement curve and hardening curves.

Fig. 1 shows the relationship between the hardening curves for fixed crack lengths and the experimental load versus displacement curve for growing crack. Assuming the deformation theory of plasticity, the hardening curve for a crack length a_i should intercept with the experimental load versus displacement curve at the point (v_i, P_i). Also, the load has been represented as a separable function of crack length and plastic displacement, and for a given crack length the power-law function has been used for describing the relation between load and plastic displacement [10–12]. In the present method, however, the 'total displacement' is used as the independent variable in the power-law function instead of the 'plastic displacement' for convenience in deriving equations. In fact, the most important point in selecting the hardening function is the capability of expressing the load versus displacement curve. Especially for most ductile materials, the fitness of the power-law function of the total displacement in expressing the hardening curve is believed to be almost the same as that based on the plastic displacement component. Considering these conditions, the hardening curve for a given crack length a_i may be expressed by

$$P(v, a_i) = P_i\left(\frac{v}{v_i}\right)^{n_i}. \tag{5}$$

In this definition, although no separate function is defined for the variables of material properties, specimen geometry, or constraint, the load P_i for a given displacement v_i is a function of those variables.

In the materials with high initiation toughness and low tearing modulus, the initial linear part of the hardening curve can not be described exactly by a power-law function of total displacement. However, the crack in

ductile materials usually proceeds with intensive plastic deformation at the crack tip beyond the initial linear elastic deformation. Therefore, the error would be very small even though the initial linear part is approximated by the power-low function such as Equation 5. Practically, the present method is focus on the relatively ductile materials revealing round hardening curves; these materials usually have relatively low initiation toughness and high tearing modulus, such as the test materials of this study.

When the load is represented as a power-law function of plastic displacement, it is generally accepted that the exponent of the power-law function is independent of crack length [10–12]. Donoso and Landes [12] showed that the exponent of hardening curve was obtainable from the Ramberg-Osgood stress-strain parameter, which is independent of crack length. However, the present method uses the total displacement v as a variable in the hardening curve instead of the plastic displacement v_p in previous definitions [10–12]. Changing the function of plastic displacement to the function of total displacement,

$$(v_p)^m = v^m(1-cP/v)^m, \tag{6}$$

where m is the constant hardening exponent [12] and c is the elastic unloading compliance. Using a least square fit, the term $(1-cP/v)^m$ can be given as a power-law function of v: βv^s, where β is a coefficient that is independent of v. Then, the term $(v_p)^m$ can be represented as

$$(v_p)^m = \beta v^{m+s}. \tag{7}$$

One can easily show that the exponent s increases as the compliance c increases (or as the crack length increases). This means that the exponent must be a variable depending on crack growth when the total displacement is used as an independent variable in the hardening function. Although the crack length is an unknown variable to be determined by iterative calculations, the displacement v_i on the experimental load-displacement data may have a relationship with the crack length a_i. Thus we can define that $s_i = s_0 + \alpha v_i$ and $n_0 = m + s_0$, where s_0 and α are constants (the values of these parameter may depend on the specimen geometry and material properties). Then the final form of the exponent n_i is written by

$$n_i = m + s_0 + \alpha v_i = n_0 + \alpha v_i. \tag{8}$$

When the exponent of the power-law function is determined, the energy ratio R_i can be easily determined from the load versus displacement data only. Inserting Equation 5 into Equations 3a and 3b, the energy ratio is expressed as follows:

$$R_i = \left(\frac{n_i+1}{n_{i+1}+1}\right)\left(\frac{P_{i+1}v_{i+1}}{P_i v_i}\right)\left(\frac{v_i}{v_{i+1}}\right)^{n_{i+1}+1}. \tag{9}$$

It is worth noting that all variables for describing the hardening curves, P_i, v_i, and n_i, can be obtained from the experimental load versus displacement curve regardless of specimen types and also the value of R_i is calculated from those variables using Equation 9. Thus the amount of crack extension can be calculated by use of above expressions as long as the J-integral formula is known for the given specimen configuration.

2.2. Crack growth in the CT and TPB specimens

For both the CT specimen and the TPB specimen, the J-integral has been evaluated from the total area under the hardening curve for crack length a_i using the η-definition of J [1, 10]:

$$J_i = \frac{\eta_i U_i}{B b_i}, \tag{10}$$

where b_i is the uncracked ligament ($=W-a_i$; W is the specimen width) and η_i is a dimensionless parameter depending on the crack length and specimen configurations:

$$\eta_i = 2 \quad \text{for TPB specimen,} \tag{11a}$$

$$\eta_i = 2 + 0.522 \times b_i/W \quad \text{for CT specimen.} \tag{11b}$$

Note that this the η-definition of J is derived based on the separation of variables in the expression of load, while the Equation 5 is an inseparable function. However, Equations 11a and 11b are used in this study without change because it can be shown that an expression for the η-factor is derived based on the inseparable function and the values are almost the same as the values from Equations 11a and 11b. This will be described in detail in a later section.

Using Equations 4 and 10, then the crack extension from i to $i+1$ is obtained as

$$\Delta a_i = \frac{b_i}{\eta_i}(1-R_i). \tag{12}$$

2.3. Crack growth in the CRB specimens

To estimate J-integral from the load versus displacement curve, we used the expression developed by Rice *et al*. [27]:

$$J_i = \frac{1}{2\pi r_i^2}\left(3\int_0^{v_i} P\,\mathrm{d}v - P_i v_i\right), \tag{13}$$

where r is the radius of uncracked ligament. Inserting Equation 5 into this equation, J_i becomes:

$$J_i = \frac{(2-n_i)}{2\pi r_i^2}U_i. \tag{14}$$

Since the increase in the crack surface is defined by $B\Delta a_i = 2\pi r_i \Delta r_i$, Equations 4 and 14 give

$$\Delta r_i = \frac{r_i}{2-n_i}(1-R_i). \tag{15}$$

3. Computational procedure and applications

3.1. Computational procedure

Fig. 2 shows the procedure of calculating the J-R curve. The input data are the experimental load versus displacement data (P_i vs. v_i data), initial and final crack

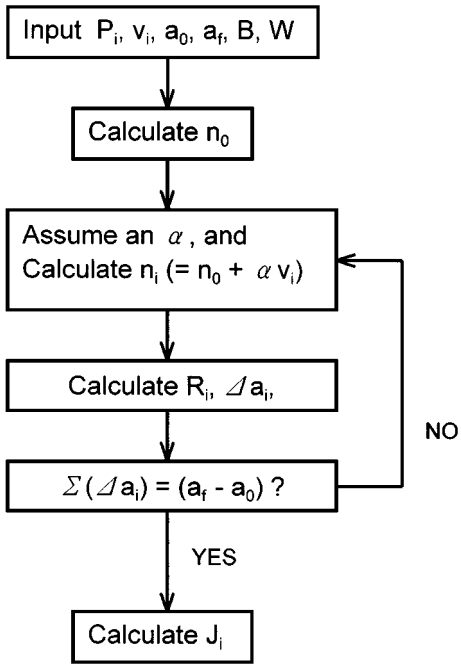

Figure 2 Calculation procedure for determining J-R curve.

lengths (or initial and final crack radii), and specimen dimensions.

The first step in the computation is to determine the value of n_0 from the experimental load-displacement data points in a small displacement range. In Equation 8, n_0 is the exponent of the hardening curve at zero load-line displacement ($v_i = 0$). However, since the load-displacement curve at nearly zero displacement is a linear region, the n_0-value obtained from this initial region is usually close to unity and can not fit the whole hardening curve for the initial crack length. This means that the load-displacement data in the linear region should be excluded in the power-law fit. Also, since the n_0-value is for the initial crack length, the regression range should be selected to assure that crack growth is negligible. In the present calculations, therefore, a displacement range is selected with a condition for plastic displacement; the n_0-value is evaluated by a power-law fit of experimental load versus displacement data which satisfy the condition of $0 < v_p(= v_i - P_i/S_0) < 0.5v_p(P_{max})$, where $v_p(P_{max})$ is the plastic displacement at maximum load P_{max}; $v_p(P_{max}) = v(P_{max}) - P_{max}/S_0$, and S_0 is the slope in the initial linear region of the experimental load-displacement curve.

The second step is an iterative calculation to determine the exponent n_i for each load-displacement point (v_i, P_i). A trial value for α in Equation 8 is assumed and the total crack extension is calculated by using the equations in the previous section. The criterion in the iterative calculation is that the calculated crack extension must be the same as the measured value:

$$\sum_{i=1}^{I} \Delta a_i = (a_f - a_0), \tag{16}$$

where I is the number of P_i-v_i data and a_0 and a_f are, respectively, the initial and final crack lengths measured by a visual method. If the total crack extension calculated can not satisfy this criterion, an alternative value of α is assumed and crack extension lengths are calculated again. This iterative calculation will be continued until the result satisfies the criterion.

The third step is to calculate the J-R curve with the hardening curves determined in the previous step. Alternatively, since the crack lengths are given for all P_i-v_i data points, the J-R curve can be determined using the expressions of the ASTM standard method [23].

3.2. Case descriptions

The proposed iteration method was applied to 10 cases for 8 different structural steels as listed in Table I [28–30]. The first 6 cases are for the CT specimens tested under static loading conditions. The cases 7 and 8 are for the TPB and CRB specimens [28] tested under static loading conditions. The TPB specimen is a Charpy size small specimen. Cases 9 and 10 are for the CT specimens tested under quasi-dynamic loading conditions [30]. All CT specimens are 20% side-grooved. The fracture tests have been performed at room temperature or at nuclear reactor operating temperature (316 °C).

For all cases, the J-R curves determined by the iteration method were compared with those measured by the conventional methods. In the quasi-static fracture testing with the CT and TPB specimens the crack length was measured by the unloading compliance method [23]. Otherwise, in the quasi-dynamic loading tests the crack length was measured by the direct current potential drop (DCPD) method [23]. For the CRB

TABLE I Summary of case descriptions [28–30]

case no.	Material	Specimen type	Test temp. (°C)	Loading condition (cross-head speed)	$W(R)$	B	$a_0(r_0)$	$a_f(r_f)$
1	SA508 Gr.3	1T-CT	*RT*	Quasi-static (1 mm/min)	50.8	25.4	27.2	30.9
2	SA508 Gr.3	1/2T-CT	*RT*	Quasi-static (1 mm/min)	25.4	12.7	14.2	17.0
3	SA508 1a	1T-CT	316	Quasi-static (1 mm/min)	50.8	25.4	30.7	35.8
4	SA508 1a Weld	1T-CT	316	Quasi-static (1 mm/min)	50.8	25.4	30.4	37.3
5	SA312 Type 347 SS	1T-CT	316	Quasi-static (1 mm/min)	50.8	25.4	31.8	36.6
6	SA312 Type 347 SS Weld	1T-CT	316	Quasi-static (1 mm/min)	50.8	25.4	32.4	38.1
7	SA533B-1	TPB	*RT*	Quasi-static (1 mm/min)	10.0	10.0	5.4	7.1
8	HSSI Weld(72 W)	CRB	0	Quasi-static (1 mm/min)	16.0		3.2	2.5
9	SA516 Gr.70	1T-CT	316	Quasi-dynamic (1000 mm/min)	50.8	25.4	29.1	38.8
10	SA516 Gr.70	1T-CT	316	Quasi-dynamic (2000 mm/min)	50.8	25.4	29.1	38.6

Note: R = specimen radius of CRB specimen, r_0 and r_f = initial and final uncracked ligament radii of CRB specimen, respectively.

specimen, the load-displacement data were read from figure in the reference [28]. In the following sections, the J-R curves, determined by the proposed method, are compared with those obtained by the conventional methods.

4. Results and discussion

4.1. CT and TPB specimen cases under static loading conditions

Figs 3 to 8 present the static J-R curves from the CT specimens. Regardless of the test materials, agreements are found between the iteration method and the standard unloading compliance method [23]. Some J-R curves determined by the unloading compliance method reveal relatively larger data scatters. These seem to have arisen from the errors in the crack length measurement by the unloading compliance method. The iteration method, however, gives smoother J-R curves.

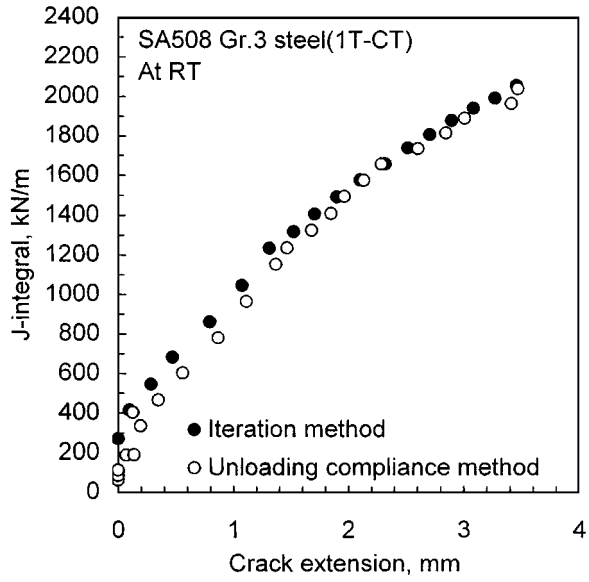

Figure 3 Comparison of J-R curves for the static test of SA508 Gr.3 steel at room temperature (1T-CT specimen).

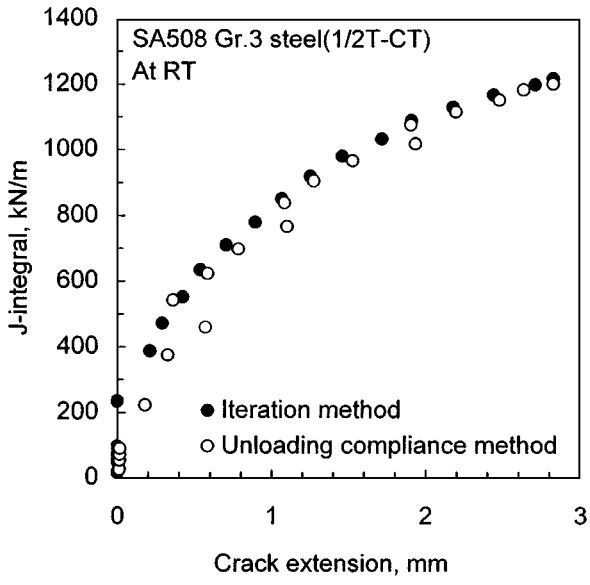

Figure 4 Comparison of J-R curves for the static test of SA508 Gr.3 steel at room temperature (1/2T-CT specimen).

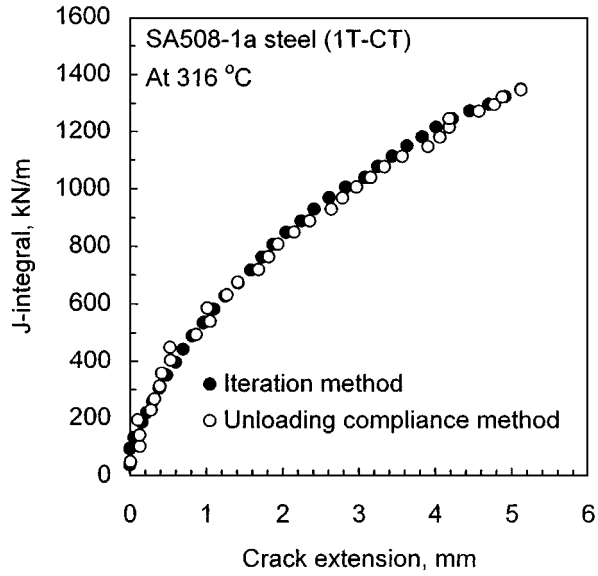

Figure 5 Comparison of J-R curves for the static test of SA508-1a steel at 316 °C (1T-CT specimen).

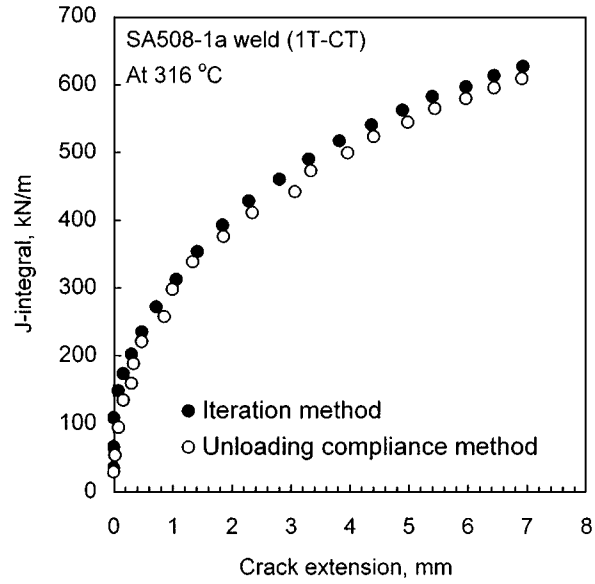

Figure 6 Comparison of J-R curves for the static test of SA508-1a steel weld at 316 °C (1T-CT specimen).

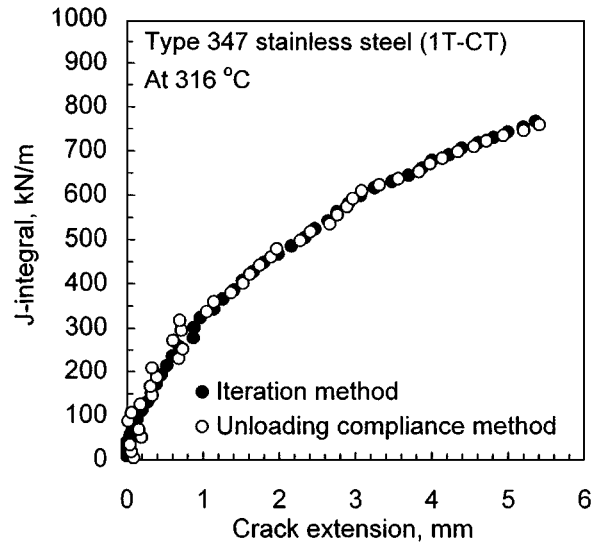

Figure 7 Comparison of J-R curves for the static test of SA312 Type 347 stainless steel at 316 °C (1T-CT specimen).

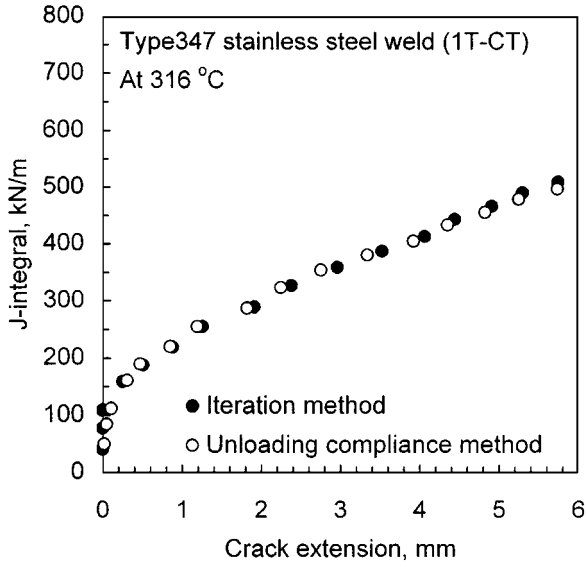

Figure 8 Comparison of J-R curves for the static test of SA312 Type 347 stainless steel weld at 316 °C (1T-CT specimen).

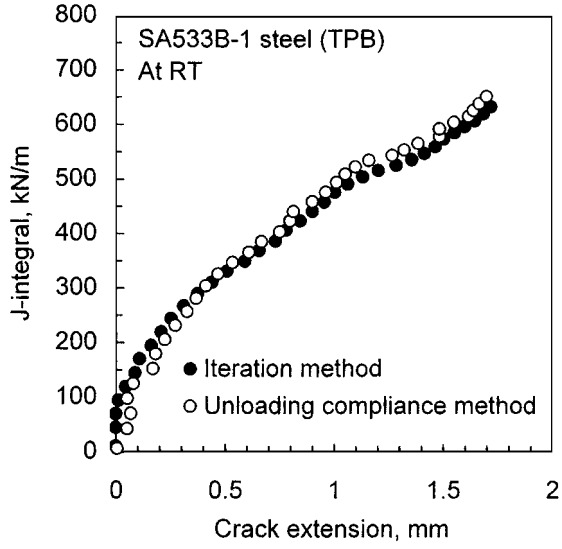

Figure 9 Comparison of J-R curves for the static test of SA533B-1 steel at room temperature (small TPB specimen).

The J-R curves for the TPB specimen are compared in Fig. 9. This result also shows an agreement between the two methods. Although the amount of crack extension is relatively small in the small TPB specimen; less than 2 mm, the J-R curve determined by the iteration method traces accurately the shape of J-R curve from the unloading compliance method.

4.2. CRB specimen case under static loading condition

For the CRB specimens, no standard method for determining the J-R curve has been established. Therefore, the J-R curve has been obtained by the multi-specimen method [28]. In Fig. 10 the J-R curve determined by the iteration method is compared with the experimental data points obtained from four specimens. The load versus displacement curve used for the present calculation was obtained from the case that had revealed the largest crack extension. In Fig. 10 J_{EXP} is the experimental value from the multi-specimen method [28] and

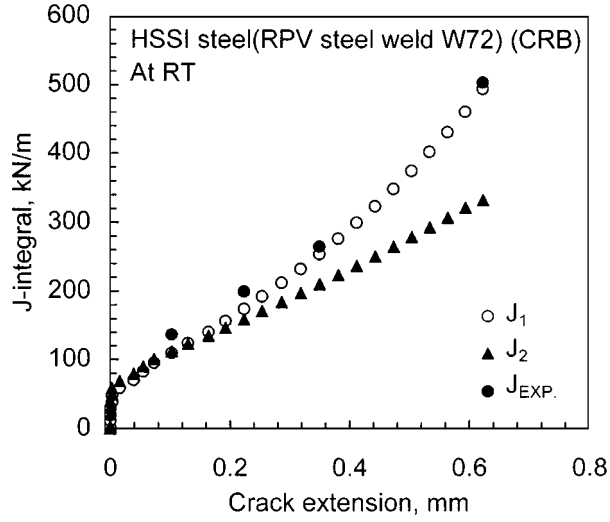

Figure 10 Comparison of J-R curves for the static test of HSSI weld (W72) at room temperature (CRB specimen) [28].

J_1 and J_2 are the data from the iteration method. In the calculations of J_{EXP} and J_1 the experimental load versus displacement curve was regarded as the hardening curve for all crack lengths [28]. However, when calculating the J_2-values, different hardening curves were used for different crack lengths. Comparing the J_1 curve with the J_{EXP}-values, it is concluded that the iteration method can be applied to the CRB specimens with sufficient accuracy.

On the other hand, the hardening curves determined by iterative calculations were used for the calculation of J_2. Fig. 10 shows that, as the crack extends, the J_2-values become smaller than the J_{EXP}- and J_1-values. This result is because the crack growth effect on the hardening curve has been ignored in the calculations of J_{EXP} and J_1. When considering the original definition of J-integral, as given by Equation 1, the J_2 curve is regarded as a more reasonable crack resistance curve.

4.3. CT specimen cases under quasi-dynamic loading conditions

For the static or quasi-dynamic cases, the DCPD method may be applicable to the measurement of crack length with sophisticated equipment [23]. In Figs 11 and 12, the J-R curves determined by the iteration method are compared with the data points estimated by the DCPD method. For the DCPD method, the data points at small crack extensions were excluded from the J-R curves. This was because it was hard to determine the valid crack growth initiation point on the DCPD-time curves. The crack length at early J-R curve is strongly dependent on the critical value of the potential drop determined as the crack growth initiation point. At larger crack extension values, however, the two methods show an agreement in the J-integral values.

4.4. The hardening curves and the hardening exponent n

Here the calculated hardening curves from the present iteration method are compared with the normalized

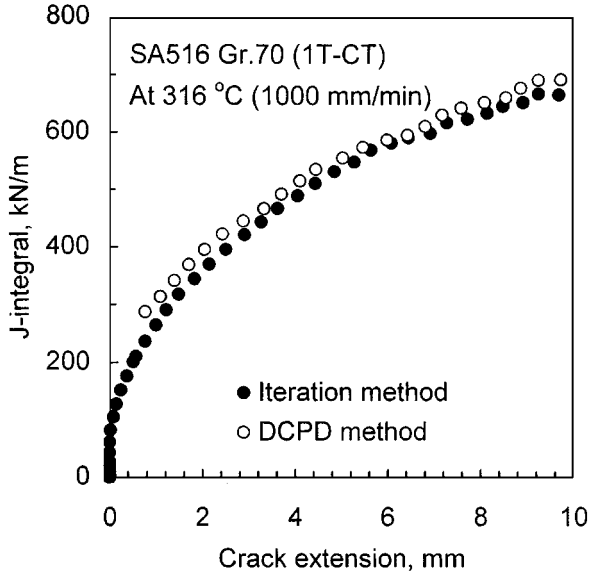

Figure 11 Comparison of J-R curves for the quasi-dynamic test of SA516 Gr.70 steel at 316 °C (1T-CT specimen, load-line displacement rate: 1000 mm/min).

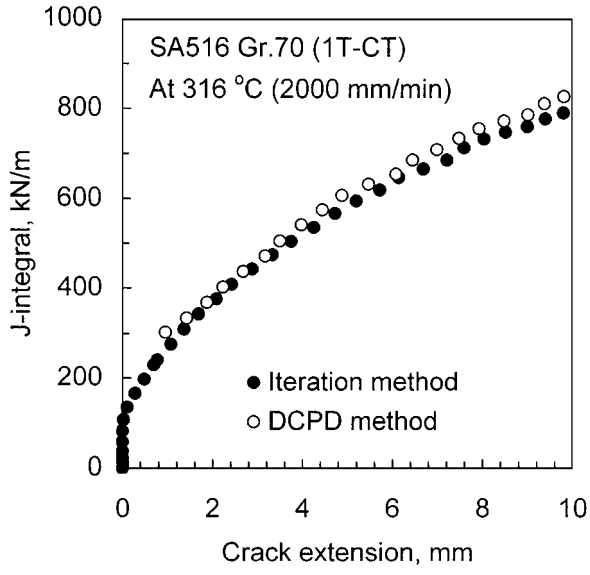

Figure 12 Comparison of J-R curves for the quasi-dynamic test of SA516 Gr.70 steel at 316 °C (1T-CT specimen, load-line displacement rate: 2000 mm/min).

load versus plastic displacement curves (P_N-v_p curves) [7–11]. In the normalization method the load P is frequently expressed by the two multiplicative functions; one is the function of crack length and the other is the function of plastic displacement:

$$P = G(a)H(v_p), \tag{17}$$

where G is a geometry-dependent function, whereas H is a material-dependent function. For a given specimen geometry, the fracture behavior may be characterized by the normalized load P_N defined by [7–12]

$$P_N = \frac{P}{G} = H(v_p). \tag{18}$$

Recently, Donoso and Landes [11, 12] proposed a Common Format Equation [CFE] approach for developing the calibration function, relating load, displacement, and crack length. They gave a systematical analyses for existing and new G function forms, and also derived simple but accurate G functions for various specimen types. For CT specimen, the G function based on the CFR approach is given by

$$G_{CT} = 1.553BW\left(\frac{b}{W}\right)^{2.236}. \tag{19}$$

For the case 5, the P_N-v_p curve was obtained from the experimental load versus plastic displacement curves using Equation 19, and then the curve was calibrated to the curves of the crack lengths of 0, 1, 3, and 5 mm: $N0.0$, $N1.0$, $N3.0$, $N5.0$ curves, respectively. Also, the hardening curves were obtained for the same crack lengths by the iteration method: $H0.0$, $H1.0$, $H3.0$, $H5.0$ curves, respectively, in which, for comparison with the N-curves, the load was represented as a function of plastic displacement. The hardening curves determined by the two methods are compared in Fig. 13. One can see that except for the small plastic displacement region of relatively large crack length cases, both the iteration method and the normalization method give similar hardening curves. The difference between the hardening curves at small displacement regions seems to have arisen from the differnce in the independent variables; v_p and v. However, the two methods produce only a small error in the area difference between the two adjacent hardening curves, and consequently very similar J-R curves will be estimated by those methods. Also, it is worth noting that the initial hardening curve, whose exponent is n_0, agrees well with the experimental load-plastic displacement curve at small plastic displacements. In Fig. 13, an arrow indicates the upper limit of the displacement range in the regression to obtain the value of n_0; $0.5v_p(P_{max})$.

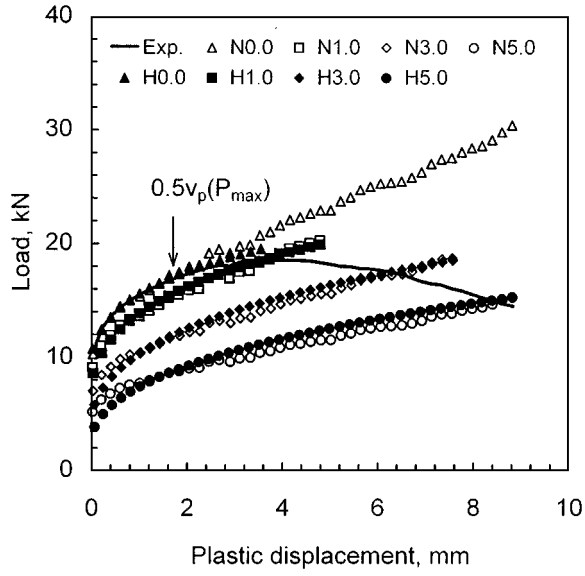

Figure 13 Comparison of the hardening curves obtained by the normalization method, Nx, and those obtained by the iteration method, Hx, where the number x means the amount of crack extension.

Table II contains the calculated exponents of hardening curves as the functions of displacement v_i. The n-value increases with displacement at the slope of α.

TABLE II The exponent of hardening curves (n) as the functions of displacement

Case no.	Specimen type	$n_i = n_0 + \alpha v_i$
1	1T-CT	$n_i = 0.15 + 0.002 v_i$
2	1/2T-CT	$n_i = 0.14 + 0.0022 v_i$
3	1T-CT	$n_i = 0.24 + 0.0025 v_i$
4	1T-CT	$n_i = 0.15 + 0.018 v_i$
5	1T-CT	$n_i = 0.18 + 0.02 v_i$
6	1T-CT	$n_i = 0.15 + 0.001 v_i$
7	TPB	$n_i = 0.18 + 0.002 v_i$
8	CRB	$n_i = 0.18 + 0.61 v_i$
9	1T-CT	$n_i = 0.15 + 0.058 v_i$
10	1T-CT	$n_i = 0.16 + 0.07 v_i$

This α-value represents the shape change of the hardening curve as the displacement v_i increases. This results from the fact that the load is defined as a function of the total displacement, as in Equation 5. As a special case, the load may be separated into the functions of v and a when $\alpha = 0$. If the load is separable, the shape of the hardening curve is independent of the crack growth, as in the definition of hardening curve based on the plastic displacement [10].

Furthermore, as presented in Table II, the exponents for CT and TPB specimens reveal a relatively weak dependency on the displacement. Whereas the exponent of CRB specimen reveals relatively strong dependency on the displacement; a large value of α, 0.61, was obtained for this specimen. This result seems to result from the different loading modes between the specimens; the bending mode is dominant in the CT and TPB specimens, otherwise the tensile mode is dominant in the CRB specimen. This implies that the tensile mode of load produces a higher α-value.

4.5. The η-factor with the function of total displacement

It has been known that the separation of variables is required to derive the η-definition of J [1, 10]. However, since the present approach is based on the definition that the exponent of power-law hardening curve is crack length dependent, as in Equation 8, the load can not be expressed as separate functions of crack length and displacement. In order to find the effect of the inseparability of variables on the value of η, we tried to derive the η-factor with the hardening exponent depending on the crack length. Using Equations 3a and 5, the J-integral, Equation 1, becomes

$$J_i = -\frac{1}{B}\left[\frac{1}{C_i}\frac{\partial C}{\partial a}\bigg|_{v_i} + \left(\ln v_i - \frac{1}{1+n_i}\right)\frac{\partial n}{\partial a}\bigg|_{v_i}\right] U_i, \tag{20}$$

where $C_i = P_i / v_i^{n_i}$. This equation implies that the η-factor for crack length a_i should be

$$\eta_i = -\left[\frac{b_i}{C_i}\frac{\partial C}{\partial a}\bigg|_{v_i} + b_i\left(\ln v_i - \frac{1}{1+n_i}\right)\frac{\partial n}{\partial a}\bigg|_{v_i}\right], \tag{21}$$

where the values of derivatives may be obtained with the finite difference forms:

$$\frac{\partial C}{\partial a}\bigg|_{v_i} = \frac{C_{i+1} - C_i}{a_{i+1} - a_i}, \tag{22a}$$

$$\frac{\partial n}{\partial a}\bigg|_{v_i} = \frac{n_{i+1} - n_i}{a_{i+1} - a_i}. \tag{22b}$$

For the cases of CT and TPB specimen cases, the values of η_i were calculated using both the expressions in Equations 11 and 21 and the results are compared in Table III. It is found that both the expressions give almost the same values. Therefore, we can conclude that the use of the inseparable function does not violate the basis of the η-definition of J, and consequently both the expressions, Equations 11 and 21, can be used for calculating the value of η.

5. Summary and conclusion

An iteration method has been developed for determining the J-R curve from the load versus load-line displacement record only. The iteration method and application results are summarized as follows:

TABLE III Comparison of η-values at representative crack length to width ratios

Case no.	Specimen type	Loading condition (cross-head speed)	a_0/W	a/W	η_a by Equation 11	η_b by Equation 21	Ratio (η_b/η_a)
1	1T-CT	Quasi-static (1 mm/min)	0.535	0.537	2.242	2.244	1.001
				0.561	2.229	2.230	1.000
				0.580	2.219	2.219	1.000
3	1T-CT	Quasi-static (1 mm/min)	0.604	0.609	2.204	2.227	1.011
				0.641	2.187	2.190	1.001
				0.701	2.156	2.155	1.000
5	1T-CT	Quasi-static (1 mm/min)	0.628	0.629	2.194	2.288	1.043
				0.665	2.175	2.165	0.995
				0.730	2.141	2.114	0.987
7	TPB	Quasi-static (1 mm/min)	0.538	0.539	2.000	1.996	0.998
				0.622	2.000	2.049	1.025
				0.707	2.000	1.991	0.996
9	1T-CT	Quasi-dynamic (1000 mm/min)	0.573	0.587	2.216	2.271	1.025
				0.666	2.174	2.180	1.003
				0.758	2.126	2.092	0.984

(1) In the iteration method, the hardening curve is described by a power-law function, in which the exponent is given as a linear function of load-line displacement. For each crack length, the hardening curve is determined by iterative calculation method. The iterative calculation is continued until the total amount of crack extension becomes equal to the measured crack extension. Finally, the J-integral values are calculated from the hardening curves and crack lengths are determined in the iterative calculation step.

(2) The method developed was successfully applied to the static J-R tests using CT, TPB, and CRB specimens and to the quasi-dynamic J-R tests using CT specimens. The iteration method can be regarded as an alternate method that can be applied to any specimen types and to any loading rates.

(3) The calculated hardening curves were compared with the calibrated curves obtained by use of a normalization method. The two methods gave very similar curves. It was also shown that the values of η evaluated based on the inseparable function for load were almost the same as the values from the conventional expression for η which is drawn from a separable function.

Acknowledgement

This work has been carried out as a part of the Reactor Pressure Boundary Materials Project that has been financially supported by MOST in Korea.

References

1. H. A. ERNST, P. C. PARIS and J. D. LANDES, Fracture Mechanics: Thirteenth Volume, ASTM STP 743, 1981, pp. 476–502.
2. H. A. ERNST, P. C. PARIS, M. ROSSOW and J. W. HUTCHINSON, Fracture Mechanics, ASTM STP 677, edited by C. W. Smith, 1979, pp. 581–599.
3. J. A. JOYCE, H. A. ERNST and P. C. PARIS, Fracture Mechanics: Twelfth Volume, ASTM STP 700, 1980, pp. 222–236.
4. K. BRUNINGHAUS, J. FALK, M. TWICKLER and W. DAHL, *Eng. Frac. Mech.* **34** (1989) 989–1000.
5. X. SUN, Z. SUN, X. HUA and Z. TIAN, *ibid.* **52** (1995) 901–905.
6. J. D. LANDES and R. HERRERA, *Int. J. Fracture* **36** (1988) R9–R14.
7. *Idem., ibid.* **36** (1988) R15–R20.
8. R. HERRERA and J. D. LANDES, *J. Test. Eval.* **16** (1988) 427–449.
9. R. WONG, R. HERRERA, Z. ZHOU and J. D. LANDES, *Eng. Frac. Mech.* **37** (1990) 153–161.
10. M. H. SHAROBEAM and J. D. LANDES, *Int. J. Fracture* **47** (1991) 81–104.
11. J. R. DONOSO and J. D. LANDES, *Eng. Frac. Mech.* **47** (1994) 619–628.
12. *Idem., ibid.* **54** (1996) 499–512.
13. J. D. LANDES, Z. ZHOU, K. LEE and R. HERRERA, *J. Test. Eval.* **19** (1991) 305–311.
14. K. LEE and J. D. LANDES, Fracture Mechanics: Twenty-Forth Sympsium, ASTM STP 1207, edited by J. D. Landes, D. E. McCabe and J. A. M. Boulet, 1994, pp. 422–446.
15. C. J. F. O. FORTERS and F. L. BASTIAN, *J. Test. Eval.* **25** (1997) 302–307.
16. J. M. HU, P. ALBRECHT and J. A. JOYCE, Fracture Mechanics: Twenty-Second Symposium (Vol. 1), ASTM STP 1311, edited by H. A. Ernst, A. Saxena, D. L. McDowell, 1992, pp. 880–903.
17. X. CHEN, P. ALBRECHT, W. BRIGHT and J. JOYCE, Special Applications and Advanced Techniques for Crack Size Determination, ASTM STP 1251, edited by J. J. Ruschau and J. K. Donald, 1995, pp. 83–103.
18. B. S. LEE, J. H. YOON and J. H. HONG, *Eng. Frac. Mech.* (1997), submitted.
19. E. P. ASTA and E. CHOMIC, *Nucl. Eng. Design* **160** (1996) 129–135.
20. B. H. KIM and C. R. JOE, *Eng. Frac. Mech.* **34** (1989) 221–231.
21. A. MARTINELLI and S. VENZI, *ibid.* **53** (1996) 263–277.
22. A. SAXENA and S. J. HUDAK, JR., *Int. J. Fracture* **14** (1978) 453–468.
23. ASTM E 1737-96, Standard Test Method for J-Integral Characterization of Fracture Toughness, 1996, pp. 67–90.
24. J. R. RICE, in "Fracture," Vol. 2, edited by H. Liebowitz (Academic Press, New York, 1968) pp. 191–311.
25. Y. LIU, X. LI and X. TAO, *Int. J. Pres. Ves. & Piping* **31** (1988) 157–164.
26. H. MA, Z. WANG and L. ZHU, *Int. J. Fracture* **68** (1994) 45–54.
27. J. R. RICE, P. C. PARIS and J. C. MERKLE, Progress in Flow Growth and Fracture Toughness Testing, ASTM STP 536, (ASTM, Philadelphia, 1973) pp. 231–245.
28. J. H. GIOVANOLA, R. W. KLOOP, J. E. CROKER, D. J. ALEXANDER, W. W. CORWIN and R. K. NANSTAD, in Small Specimen Test Technique, ASTM STP 1329, edited by W. R. Corwin, S. T. Rosinski and E. van Walle, 1997, in press.
29. J. H. HONG *et al.*, Fracture resistance (J-R curve) characteristics of primary piping materials for Yong-Gwang 3/4 nuclear power plants, Report no: KAERI/RM-21/91, Korea Atomic Energy Research Institute, 1991.
30. B. S. LEE *et al.*, Evalution of DSA effects on SA516-Gr.70 steel for reactor coolant piping elbow material (dynamic and quasi-static J-R characteristics), Report no: KAERI/CR-043/97, Korea Atomic Energy Research Institute, 1997.

Received 21 October
and accepted 16 November 1998